ARCHIVES OF ELECTRICAL ENGINEERING VOL. 73(4), pp. 1013–1023 (2024)

DOI 10.24425/aee.2024.152108

Approximation of electromagnetic force axial distribution in "single excitation coil – permanent magnet runner" module based on modified Kloss function

SEBASTIAN JAN BARTEL ✉, KRZYSZTOF KLUSZCZYŃSKI

Cracow University of Technology
Warszawska 24, 31-155 Kraków, Poland
e-mail: {✉ sebastian.bartelkrzysztof.kluszczynski}@pk.edu.pl

(Received: 22.04.2024, revised: 22.11.2024)

Abstract: An elementary part of various electromagnetic devices or linear electric machines is a module consisting of an excitation coil and a permanent magnet (PM runner). The electromagnetic force axial distribution in this "single excitation coil – PM runner" module is usually determined by numerical field calculations at discrete runner positions. When solving the mathematical model, a table containing discrete values of the electromagnetic force axial distribution is usually used (the so-called lookup table).

The authors of this article decided to find a simple analytic function that approximates the calculated discrete electromagnetic force function with technically sufficient accuracy and the smallest possible number of coefficients. After many attempts, they proposed the modified Kloss function with 2 coefficients denoted as S' and M', the values of which for the best approximation have to be determined using the optimization algorithm e.g. the Hooke–Jeeves algorithm. This analytical function reflects perfectly the nature of the discrete electromagnetic force axial distribution determined by the numerical field calculations and approximates the discrete function with fully satisfactory accuracy.

Key words: approximation of discrete electromagnetic force axial distribution, electromagnetic pump, "excitation coil – PM runner" module, Kloss function, linear PM machine

1. Introduction

A consequence of the dynamic development of a high-energy permanent magnet manufacturing technology is the increasing spread of a rotary and linear PM (permanent magnet) motor in various industrial applications [5, 7, 9–13]. This entails the development of increasingly accurate

mathematical models, as well as the improvement of methods for their quick and effective solution, which is of significant importance, both in the design process of these motors, as well as in their different applications, especially in the development of new control strategies.

An elementary part of various electric devices and linear electrical motors is the module consisting of an excitation coil (fed by excitation current I) mounted on a cylinder made of non-magnetic material (e.g. polymer, 3D printer filament, Teflon etc.) and a ring-shaped or disc-shaped permanent magnet placed inside the cylinder, capable of moving along its z_R-axis in a reciprocating motion under the electromagnetic force $F(z_R, I)$. Such an elementary "single excitation coil – PM runner" module presented in Fig. 1 can be found, for example, in a compact electromagnetic pump, shown in Fig. 2 and described in detail in [2–4].

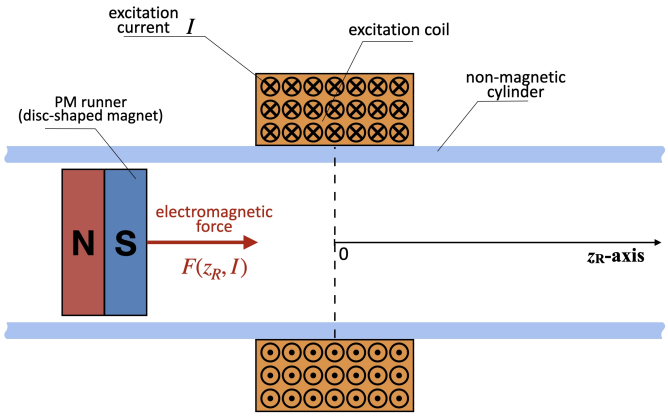

Fig. 1. Elementary "single excitation coil – PM runner" module with disc-shaped permanent magnet (cross-section)

This compact electromagnetic pump is created by integrating a conventional cylindrical piston pump with an electric linear motor. The permanent magnet performs two functions simultaneously: the function of a runner (which operates depending on the control strategy as a synchronous or step motor) and the function of the pump's piston. As seen in Fig. 1, the electromagnetic force $F(z_{R,I})$ acting between the excitation coil and the permanent magnet is a function of 2 variables: the position of the runner on the z_R-axis and the value of the excitation current I. Since the considered module does not contain ferromagnetic elements (the permeability of the whole system under consideration is μ_0), it can be treated as a linear magnetic circuit, and the consequence of that is a significant simplification of the notation of the electromagnetic force:

$$F\left(z_{R,I}\right) = \frac{I}{I_{\max}} f\left(z_{R,I} = I_{\max}\right), \tag{1}$$

where $I_{\max}$ is the maximum allowable current in the excitation coil.

The function $f\left(z_{R,I} = I_{\max}\right)$ can be given in tabular or graphical form based on numerical field calculations or measurements as a discrete function defined on a set of properly selected points distributed along the z_R-axis. When solving a mathematical model, this table is considered an integral part of the model and is known as the electromagnetic force lookup table [1, 5, 6, 9, 14].

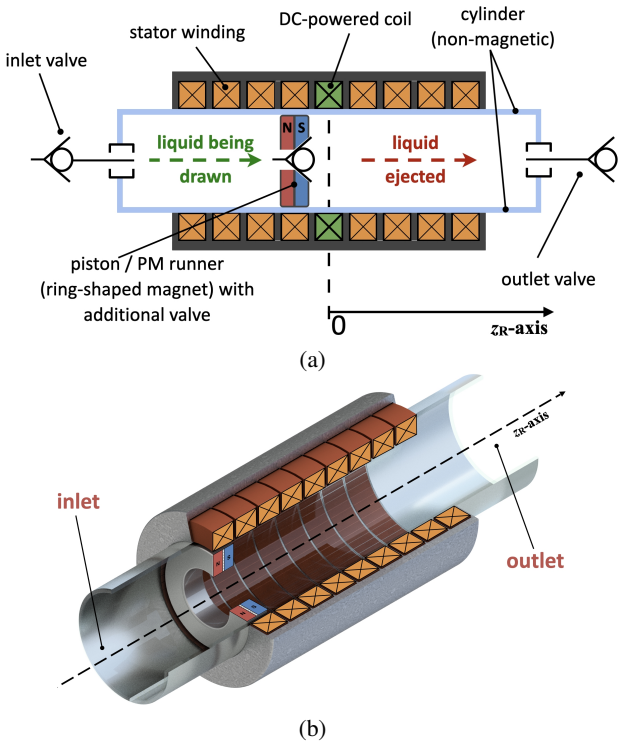

Fig. 2. Compact electromagnetic pump with ring-shaped magnet: schematic representation of the pump (cross-section) (a); 3D visualization (b)

The purpose of this article is to find the simple analytic function (mathematical approximation) with the smallest possible number of coefficients that best represents the nature of this discrete function and best approximates its shape in terms of RMSE (root-mean-square error).

2. Determination of discrete electromagnetic force axial distribution

As known, the discrete electromagnetic force axial distribution can be easily determined on the basis of numerical field calculations. Let us make it using the example of a designed and constructed prototype of the electromagnetic pump depicted in Fig. 2. The main geometrical and winding data of the elementary "single excitation coil – PM runner" module are, as follows: length of the excitation coil $L_C = 10$ mm, height of the excitation coil (difference between external and internal radius) $T_C = 10$ mm, length of the PM runner $L_R = 10$ mm, height of the PM runner (difference between external and internal radius) $T_R = 9$ mm, thickness of the cylinder $T = 1.6$ mm and the number of excitation coil turns $n = 576$. It is noteworthy that the determination of the proper proportion of the excitation coil (length of the coil to its height) in the constructed prototype was the subject of separate considerations presented in [3,4].

The excitation coil is made of insulated winding wires AWG 26 (American wire gauge) with a diameter equal to 0.4 mm and the percentage filling factor of the coil reaches the value 74%. Geometric dimensions for the module under consideration are summarised in Fig. 3(a). The cylinder is made of a Teflon material and the permanent magnet is manufactured with neodymium material N38. Based on knowledge of the insulation class, winding wire diameter and cooling conditions, the excitation current density was chosen to be 4 A/mm^2, which corresponds to a maximum value of the excitation current $I_{\max}$ equal to 0.7 A ($I_{\max} = 0.7$ A).

The spatial distribution of the magnetic field at the example position $z_R = -25$ mm is shown in Fig. 3(b). The value of the electromagnetic force acting on the runner at this position is equal to

$$F\,(z_R = -25 \text{ mm}, I_{\max} = 0.7 \text{ A}) = 1.48 \text{ N}.$$

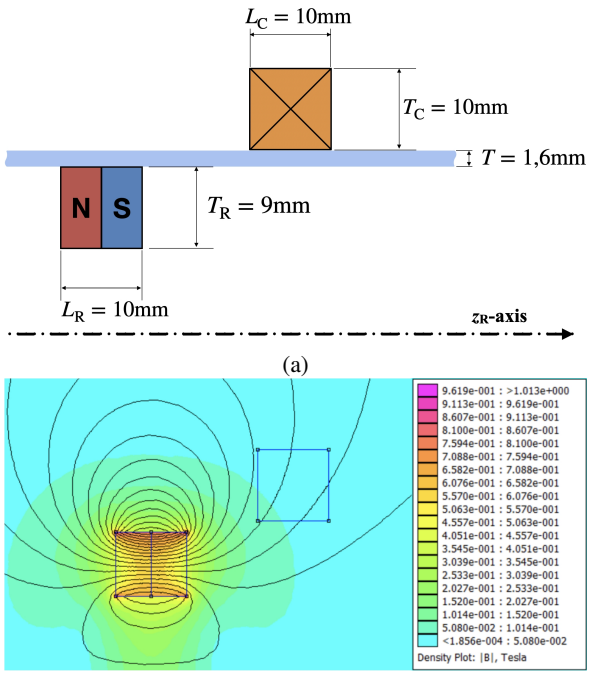

Fig. 3. Elementary "single excitation coil – PM runner" module of the electromagnetic pump (axisymmetric cross-section): geometric dimensions (a); spatial distribution of magnetic field (b)

In a further step, the values of the electromagnetic force acting on the runner were determined in the range from –80 mm to 80 mm with a discretisation step $\Delta z_R = 0.5$ mm. This means that the values of the electromagnetic force had to be calculated at 320 points (point 1 corresponds to a runner position $z_R = -80$ mm and point 320 corresponds to a runner position $z_R = 80$ mm). The values of the electromagnetic force (at excitation current $I_{\max} = 0.7$ A) in the selected points: 1, 2, 3, . . . 141, 142, 143, 144, 145, 146, 147 (the neighbourhood of the positive maximum value), . . . 318, 319, 320 are gathered in Table 1.

Table 1 corresponds to the graphical form given in Fig. 4, presenting the discrete function of the electromagnetic force.

Table 1. Electromagnetic force (at excitation current $I_{\max} = 0.7$ A) in the range from $z_R = -80$ mm to $z_R = 80$ mm with the discretization step $\Delta z_R = 0.5$ mm (values given for the selected points: 1, 2, 3, . . . 141, 142, 143, 144, 145, 146, 147, . . . 318, 319, 320)

Point number	**Electromagnetic force F [N]**
1	0.0703
2	0.0718
3	0.0733
⋮	⋮
141	4.8370
142	4.9391
143	5.0112
144	5.0483
145	5.0451
146	5.0029
147	4.9204
⋮	⋮
318	–0.0732
319	–0.0718
320	–0.0703

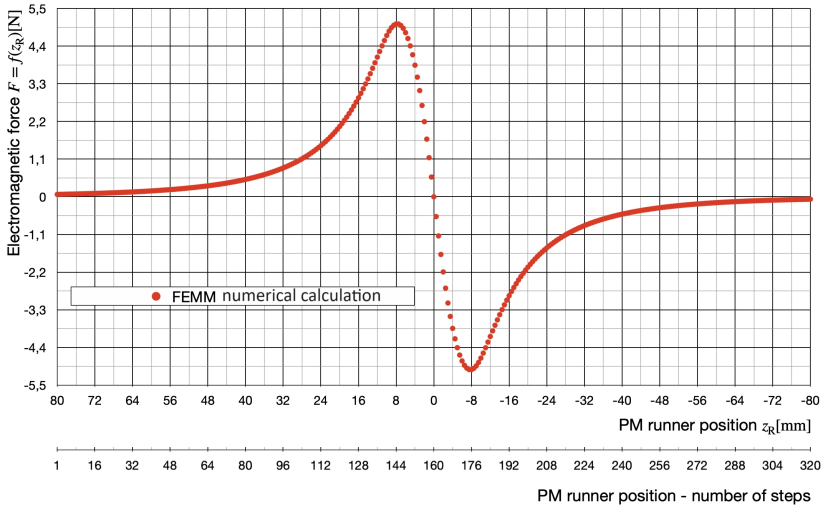

Fig. 4. Discrete values of electromagnetic force axial distribution determined on the basis of numerical field calculations in the range from –80 mm (step number 1) to 80 mm (step number 320) with a discretisation step $\Delta z_R = 0.5$ mm at the excitation current $I_{\max} = 0.7$ A

3. Mathematical approximation of the discrete electromagnetic force function

In the physical sciences, various special functions are known to describe selected features of physical phenomena. Often these functions are named after the scientists who proposed their use: the Boltzmann function, Cauchy function, Fermi–Dirac function, Gaussian function, Lorentz function etc. It turns out that such functions can also find applications in technical sciences, for with their help it is also possible to describe many phenomena and processes occurring in technical devices. An interesting example of the use of the Fermi–Dirac function to describe the behaviour of a linear SMA actuator can be found in [8]. So, not surprisingly, it was decided to start the search for an approximation function from the above-mentioned functions. Guided by the similarity of the difference between 2 Gaussian functions to the function given in Fig. 4 it is first proposed to consider the following anti-symmetric function containing 3 coefficients A, B, C:

$$f(z_R) = A \cdot e^{\left(\frac{-(z_R+B)^2}{C^2}\right)} - A \cdot e^{\left(\frac{-(z_R-B)^2}{C^2}\right)}. \tag{2}$$

The influence of coefficients A, B and C on the shape of this function is illustrated in Fig. 5. Parameter A changes the maximum/minimum values of the function, while changes in coefficients B and C (shifting the function along the z-axis and changing the slope of the function branches) are accompanied by a concomitant change in the maximum/minimum value of the function.

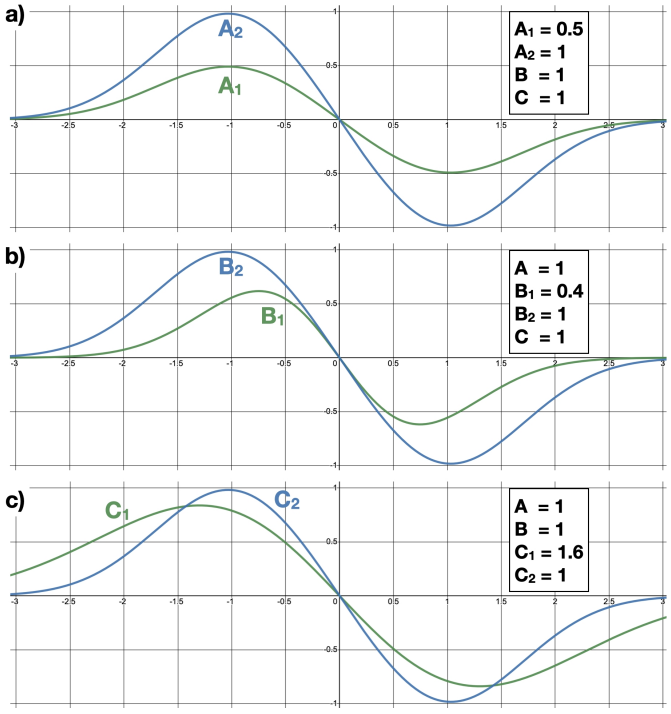

Fig. 5. Influence of coefficients A, B and C on the shape of the function described by Eq. (2)

To determine coefficients A, B and C at which the function given by Eq. (2) best approximates the function $f\left(z_{R,I} = I_{\max}\right)$ from Fig. 4, the Hooke–Jeeves optimisation algorithm was used, aiming to minimise RMSE resulting from the differences among the 320 discrete electromagnetic force values determined by the numerical field calculations (Fig. 4) and the corresponding 320 values of the approximation function described by Eq. (2).

The values of coefficients A, B and C are, respectively, 65.27, 0.60 and 13.51, and the result of the approximation is presented in graphical form in Fig. 6. The RMSE for the considered range of the runner position $z_R = [-80, 80]$ mm is 0.434, and the percentage error is: $\epsilon = 35.3\%$. Such a discrepancy was considered too large and the number of coefficients too high.

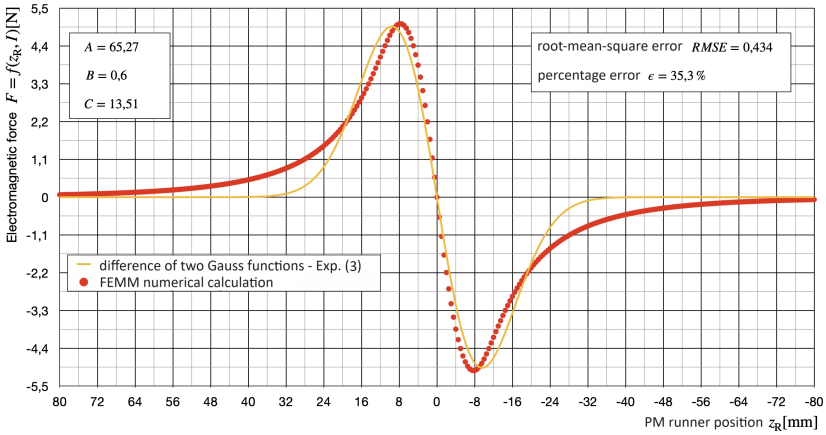

Fig. 6. Approximation of the discrete function of the electromagnetic force by the function described by the difference of two Gauss functions Eq. (2)

The next function chosen to be considered because of its similarity to the discrete electromagnetic force function presented in Fig. 4 was the Kloss function. The function is named after its creator, professor at the Royal University of Technology in Berlin, Max Kloss (1873–1961). He proposed the expression, which describes very well the electromagnetic torque T_e developed by the asynchronous machine versus the slip s:

$$T_e(s) = \frac{2T_k}{\frac{s}{s_k} + \frac{s_k}{s}}, \tag{3}$$

where T_k is the pull-out torque and s_k is the pull-out slip.

After introducing 2 coefficients denoted as M and S and replacing the variable s with the variable z_R, the basic form of this new approximation function was obtained:

$$f(z_R) = \frac{M}{\frac{z_R}{S} + \frac{S}{z_R}}. \tag{4}$$

As seen in Fig. 7, the parameter M changes the maximum value without changing its position along the z_R-axis. Regarding the parameter S, its variation affects the slope of the function branches without changing the maximum value.

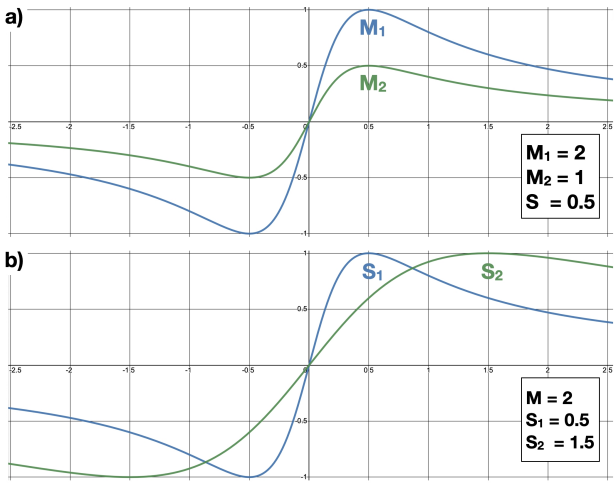

Fig. 7. Influence of the coefficients M and S on the shape of the base form of Kloss function

To determine the coefficients M and S at which the function given by Eq. (4) best approximates the function $f\left(z_{R,I} = I_{\max}\right)$ from Fig. 4, the Hooke–Jeeves optimisation algorithm (the same as in the previous case) was used. The values of the coefficients M and S are, respectively, (–8.77) and 4.89, and the result of the approximation is presented in graphical form in Fig. 8. The RMSE for the considered range of the runner position $z_R = [-80, 80]$ mm is 0.572, and the percentage error is: $\epsilon = 46.5\%$. These errors are obviously too high.

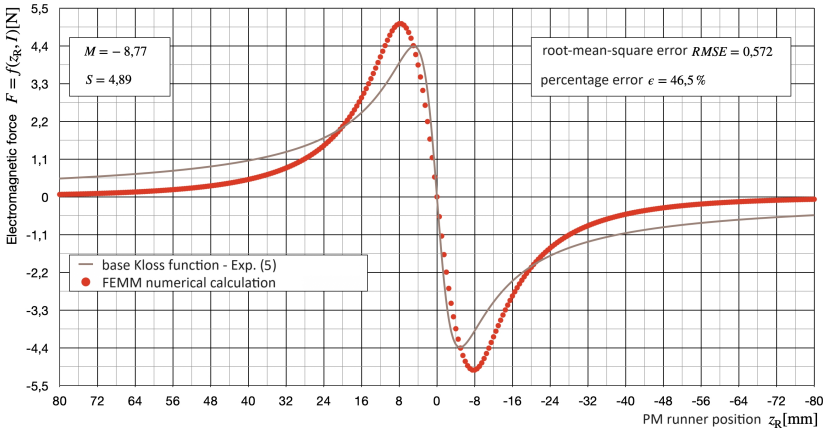

Fig. 8. Approximation of the electromagnetic force as a function of runner position z_R (with $I = I_{\max}$) using the Kloss function

In addition, the maximum force value is too low and the function converges asymptotically too slowly to the z_R-axis as the coordinate z_R approaches $+\infty$ and $-\infty$ but, as seen in Fig. 8, the approximation function closely matches the values of the electromagnetic force in the interval from $z_R = [-4, 4]$ mm, which is of key importance for the behaviour of a runner operating at a given control strategy.

So, bearing this convenience in mind, after many attempts it is proposed to modify the Kloss function to the following form:

$$f(z_R) = \frac{\dfrac{M}{z_R}}{\left(\dfrac{z_R}{S} + \dfrac{S}{z_R}\right)^2} = \frac{MS^2 z_R}{\left(S^2 + z_R^2\right)^2}. \tag{5}$$

The changes made are highlighted in red. The result of the approximation obtained with the use of the modified Kloss function given by Eq. (5) is shown in Fig. 9. The coefficients M and S, chosen in the same way as earlier, are: $M = (-199.89)$ and $S = 13.12$. The RMSE is equal to 0.054, while the percentage error has decreased to $\epsilon = 4.4\%$. This result was considered to be fully satisfactory.

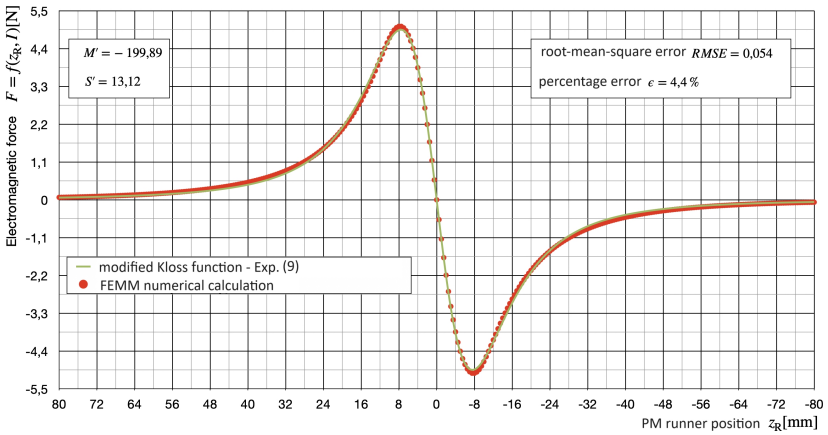

Fig. 9. Approximation of the electromagnetic force as a function of runner position z_R (with $I = I_{\max}$) using the modified Kloss function

It is easy to notice that this will be convenient to simplify the notation of the modified Kloss function by making the following substitution:

$$S^2 = S', \tag{6}$$

$$MS^2 = M'. \tag{7}$$

So, its final general form is:

$$f(z_R) = \frac{M' z_R}{\left(S' + z_R^2\right)^2}. \tag{8}$$

The above approximation function has the required simple structure and includes only 2 coefficients. In this form, the newly introduced coefficients take the values: $M' = (-34387)$ and $S' = 172$.

According to Eq. (1) the electromagnetic force axial distribution in the elementary "single excitation coil – PM runner" module with the geometrical dimensions given in Fig. 3(a), can be described analytically by the following function of 2 variables:

$$F\left(z_{R,I}\right) = \frac{I}{I_{\max}} \cdot \frac{M' z_R}{\left(S' + z_R^2\right)^2} = \frac{I}{0.7} \cdot \frac{(-34387) \cdot z_R}{\left(172 + z_R^2\right)^2}. \tag{9}$$

The shape of this 2-variable function in the form of a 3D diagram is shown in Fig. 10.

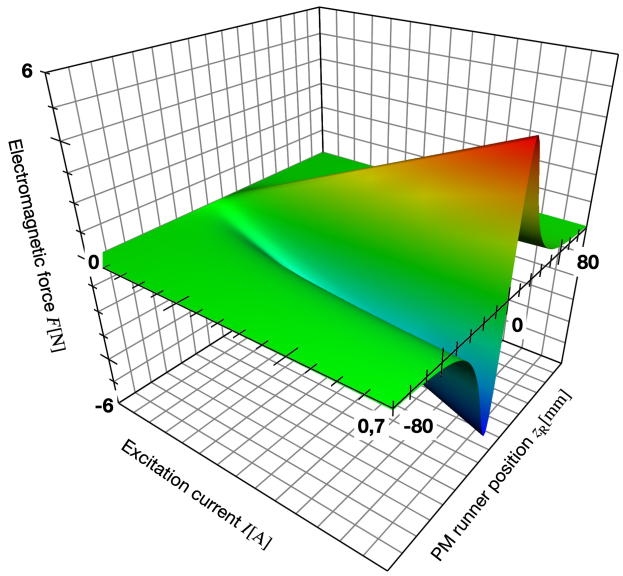

Fig. 10. Electromagnetic force as a function of 2 variables: the position of the runner z_R and excitation current I in 3D space

The great advantage of the approach presented above is that, when solving a mathematical model of an electromagnetic device containing the elementary "single excitation coil – PM runner" module or series of such elementary modules, it is possible to replace the discrete electromagnetic force axial distribution given in tabular form or graphical form (see example table – Table 1 and example figure – Fig. 4) by an analytic continuous function with only 2 coefficients M' and S' (Eq. (8)) the values of which have to be determined using the optimisation algorithm e.g. the Hooke–Jeeves algorithm.

4. Conclusions

The modified Kloss function shown in Eq. (8) and containing only 2 coefficients, describes very well the shape of the discrete function related to the electromagnetic force in an elementary "single excitation coil – PM runner" module. It reflects perfectly the nature of the discrete electromagnetic force axial distribution determined by the numerical field calculations and approximates discrete functions with fully satisfactory accuracy.

The use of the approximation function allows the electromagnetic force lookup table (similar to Table 1) to be eliminated from the mathematical model of the "single excitation coil – PM runner" module (or from a mathematical model of any electromagnetic device or linear electric motor composed of such modules) and enables this mathematical model to be converted into a purely analytical model.

References

[1] Barba P.D., Savini A., Wiak S., *Field models in electricity and magnetism*, Springer (2008), DOI: 10.1007/978-1-4020-6843-0.

[2] Bartel S., Kluszczyński K., Pilch Z., *Concept of electromagnetic periodical duty pump with programmable liquid flow*, 15th Selected Issues of Electrical Engineering and Electronics, Zakopane, Poland (2019), DOI: 10.1109/WZEE48932.2019.8979673.

[3] Bartel S., Kluszczyński K., *The problem of choosing the optimal ratio: height to length of excitation coil in linear cylindrical PM synchronous motors*, Przegląd Elektrotechniczny (in Polish), vol. 248, no. 2, pp. 1–7 (2023), DOI: 10.15199/48.2024.02.10.

[4] Bartel S., Kluszczyński K., Pilch Z., *The Influence of a Linear Steel Screw and a Linear Nylon Screw Upon Measuring Electromagnetic Force in a Cylindrical PM Synchronous Motor*, 2023 Progress in Applied Electrical Engineering (PAEE), Koscielisko, Poland, pp. 1–4 (2023), DOI: 10.1109/PAEE59932.2023.10244562.

[5] Bernat J., Kołota J., Stępień G., Szymański G., *An inductance lookup table application for analysis of reluctance stepper motor model*, Archives of Electrical Engineering, vol. 60, no. 1 (2011), DOI: 10.2478/v10171-011-0002-y.

[6] Domin J., Kluszczyński K., *Hybrid pneumatic-electromagnetic launcher – general concept, mathematical model and results of simulation*, Przegląd Elektrotechniczny, R. 89, no. 12, pp. 21–25 (2013).

[7] Glinka T., *Permanent magnet induction electric machines*, Wydawnictwo WNT (in Polish) (2018).

[8] Kluszczyński K., Kciuk M., *Analytical description of SMA actuator dynamics based on Fermi–Dirac function*, Acta Physica Polonica Series A, vol. 131, no. 5, pp. 1274–1279 (2017), DOI: 10.12693/APhysPolA.131.1274.

[9] Wiak S., Napieralska-Juszczak E., *Computer field models of electromagnetic devices*, IOS Press BV (2010).

[10] Laithwaite E.R., *Linear electric motors*, Mills & Boon Limited (1971).

[11] Pawluk K., Szczepański W., *Electric linear motors*, Wydawnictwa Naukowo-Techniczne (in Polish) (1974).

[12] Gieras J.F., Shen J.X., *Modern permanent magnet electric machines: theory and control*, CRC Press – Taylor and Francis Group (2023), DOI: 10.1201/9781003103073.

[13] Pawlak A.M., *Sensors and Actuators in Mechatronics: Design and Applications*, CRC Press (2007), DOI: 10.1201/9781315221632.

[14] Loic Q., Ohsaki H., *Nonlinear abc-Model for Electrical Machines Using N-D Lookup tables*, IEEE Transactions on Energy Conversion, vol. 30, iss. 1 (2015), DOI: 10.1109/TEC.2014.2358854.